M&C 2017 - International Conference on Mathematics & Computational Methods Applied to Nuclear Science & Engineering, Jeju, Korea, April 16-20, 2017, on USB (2017)

Nuclear Data Uncertainty Propagation with the Stochastic Sampling Module in RMC

Yishu Qiu*, Guanlin Shi, Kan Wang

Department of Engineering Physics, Tsinghua University, Beijing, 100084, P.R. China
**qys12@mails.tsinghua.edu.cn*

Abstract - *In this paper, an integrated, built-in stochastic sampling module, RMC-SS, is developed in the Reactor Monte Carlo code RMC. Comparing to traditional stochastic sampling tools which take the calculation code as a black box, RMC-SS is much more user-friendly and memory-efficient. Instead of storing perturbed nuclear data library, perturbation factors are prepared and stored, which can reduce the memory consumption of storing library. After reading the nominal nuclear data library and perturbation factors, RMC automatically repeats transport or burnup calculations. Each calculation will be assigned a unique random number seed to consider the statistical uncertainty. Finally, uncertainties of results are calculated by RMC. No post processing is required. Uncertainty analyses are performed in two in two problems, a bare sphere benchmark which represents a standard Monte Carlo transport calculation, and a PWR pin cell burnup benchmark, which represents a Monte Carlo burnup calculation, with RMC-SS.*

I. INTRODUCTION

Since the benchmarks for uncertainty analysis in modelling (UAM) for design, operation and safety analysis have been put forward, an increased attention has been paid to uncertainty propagation and sensitivity analysis. The benchmarks consist of 9 steps in 3 phases [1]. Various input parameters are takin in account, especially the nuclear data. Different output response functions from steady-state stand-alone neutronics calculations to time-dependent multi-physics calculations are concerned.

Recently, the capability of performing uncertainty analysis based on sensitivity/uncertainty method has been developed in the continuous-energy Rector Monte Carlo code RMC [2]. After computing sensitivities of different response functions to different types of nuclear data based on the first-order perturbation method, their uncertainties can be obtained by the “Sandwich rules”. However, this method is restricted to transport calculation and the types of responses which could be analyzed are limited to effective multiplication factor, linear response functions and bilinear response functions. Since the current capability of sensitivity and uncertainty analysis in RMC could not fully cover the needs of the benchmarks, a stochastic sampling module based on the RMC code has been developed.

II. IMPLEMETATION OF RMC STOCHASTIC SAMPLING MODULE

A stochastic sampling module was developed in the RMC code. In order to reduce the computational effort, the fast TMC method [3] has also been adopted by RMC. The methods and features of RMC are introduced in the following section briefly.

1. Stochastic sampling method

The key to stochastic sampling method is how to obtain samples from nuclear data. There are two variants of stochastic sampling methods. The NUSS system [4] by Paul Scherrer Institute (PSI) produces perturbed ACE-formatted nuclear data files from pointwise ACE-formatted nuclear data by applying multi-group nuclear data covariance while the Total Monte Carlo (TMC) method [3] by Nuclear Research and Consultancy Group (NRG) produces perturbed ENDF-6 formatted nuclear data by varying nuclear reaction model parameters. The PSI process [5], which is shown in Fig.1, is adopted by RMC.

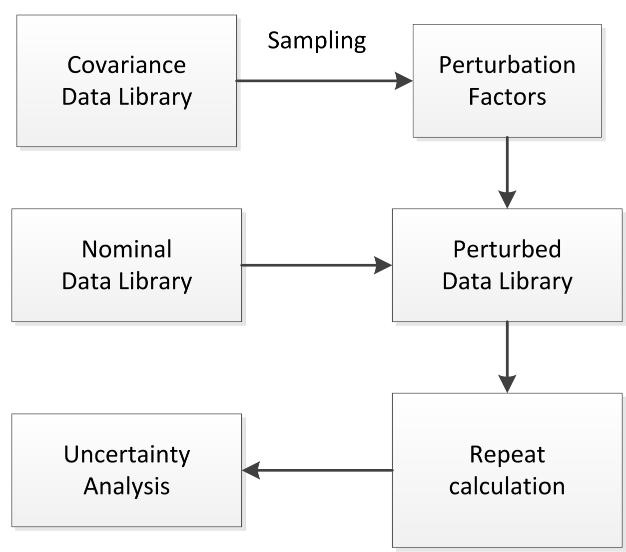

Fig. 1. Flow to perform uncertainty analysis

2. How to generate perturbation factors

As shown in Fig. 1, the first step of the stochastic sampling method is to generate perturbation factors. To do so, the relative covariance data library V is decomposed into

$$V = D^T D, \tag{1}$$

where the dimension of the relative covariance data library V is $m \times m$ and the dimension of the D is $m' \times m$ ($m' \leq m$).

The second step is to get $N \times m'$ random samples from the multivariate standard normal distributions (zero mean and unit variance) and store in the matrix Z where N is the sample size.

The third step is to get perturbation factors from

$$P = I + ZD, \tag{2}$$

where P is the matrix to store the perturbation factors and I is the matrix with every element equals to one, and the dimension of both P and I is $N \times m$.

With these perturbation factors in matrix P, N calculation can be repeated after N perturbed ACE-formatted nuclear data files can be generated by applying these perturbation factors onto the pointwise ACE-formatter nuclear data. And the uncertainty of the concerned result can be obtained by

$$\sigma^2_{observed} = \frac{1}{N-1}\sum_{i=1}^{N}(k_i - \bar{k}). \tag{3}$$

And the average value $\bar{k}$ is defined as

$$\bar{k} = \frac{1}{N}\sum_{i=1}^{N} k_i , \tag{4}$$

where k_i is the result of i -th run.

3. Fast stochastic sampling method

It should be noted that the uncertainty obtained from Eq. (3), $\sigma_{observed}$, contains both the statistical uncertainty $\bar{\sigma}_s$ and the uncertainty caused by perturbation of nuclear data, σ_d, as shown by

$$\sigma^2_{observed} \approx \bar{\sigma}^2_s + \sigma^2_d , \tag{5}$$

where

$$\bar{\sigma}^2_s = \frac{1}{N}\sum_{i=1}^{N}\sigma^2_{s,i} , \tag{6}$$

where $\sigma_{s,i}$ is the statistical uncertainty of i -th run.

In order to make $\sigma^2_{observed} \approx \sigma^2_d$, usually sufficient particle histories are required to obtain a small statistical uncertainty, e.g., $\bar{\sigma}_s \approx 5\% \times \sigma_{observed}$. As a result, it is very time-consuming to perform uncertainty analysis for criticality calculations, let alone burnup calculations.

Two methods have been put forward to reduce the computational efforts: the fast GRS method [6] and the fast TMC method. In this paper, the fast TMC method is adopted in RMC. The idea is introduced briefly as follows. The fast TMC method is based on the observation of the phenomenon that if $\bar{\sigma}_s \approx 50\% \times \sigma_{observed}$, Eq. (5) and Eq. (6) still hold.

In order to estimate $\bar{\sigma}_s$, the fast TMC method performs each calculation with a different random seed number. Therefore, the statistical uncertainty and the total uncertainty are obtained from Eq. (6) and Eq. (3). Finally, the uncertainty from nuclear data can be calculated by

$$\sigma^2_d \approx \frac{1}{N-1}\sum_{i=1}^{N}(k_i - \bar{k}) - \frac{1}{N}\sum_{i=1}^{N}\sigma^2_{s,i} . \tag{7}$$

4. New features in RMC

The traditional stochastic sampling process was shown in Fig.2. Since the code was taken as a black box, perturbed library in the standard ACE format has to be generated and calculations are repeated separately. As a result, users have to produce different input files with different random seed numbers, in order to consider the statistical uncertainty in Eq. 6. Furthermore, the uncertainties of results can only be post processed after all calculations finished.

In order to make the stochastic sampling process more user-friendly, an integrated built-in stochastic sampling module was developed in RMC code, as shown in Fig. 3. As can be seen, only one input file is required. RMC will change the random seed number at each calculation automatically. Instead of perturbed library in the standard ACE format, only perturbation factors are stored. Therefore, the memory consumption of storing library can be significantly reduces. For example, consider a nominal pointwise ACE-formatted nuclear data library is 700 Megabytes and 300 samples are required to get a converged uncertainties. The memory consumption of the perturbed nuclear data library in the standard ACE format will be 700 ×300 Megabytes≈210,000 Megabytes. However, since RMC only stores perturbation factors, consider the memory consumption of each perturbation factor file is 4 kilobytes, only 4 ×300 kilobytes≈1.2 Megabytes will be required for 300 samples.

After reading the nominal library and perturbation factors, RMC perturbs the nominal library and prepares the perturbed nuclear data for transport/burnup calculations. After all calculations finish, uncertainties are automatically calculated by RMC. No post processing are required.

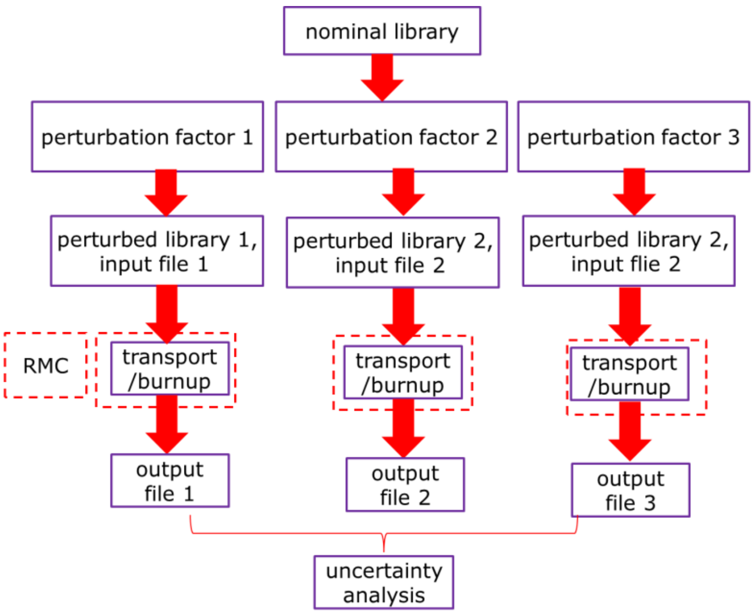

Fig. 2. Traditional stochastic sampling process

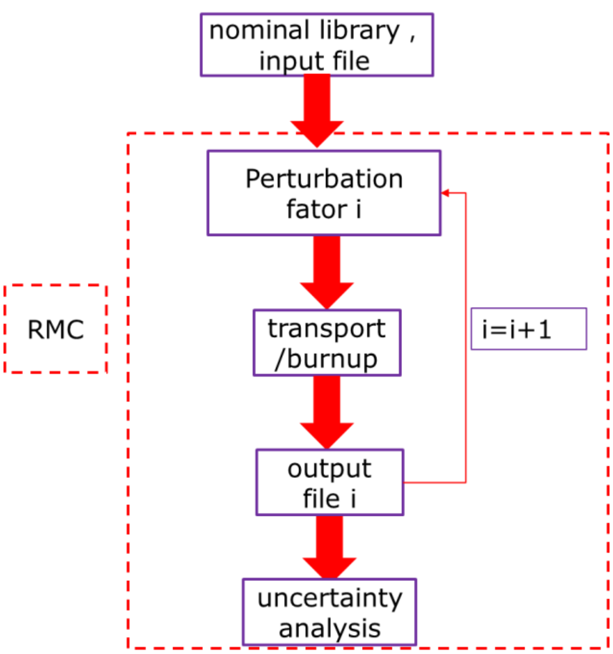

Fig. 3. RMC integrated built-in stochastic sampling module

III. RESULTS

1. Transport Calculation

Uncertainty analysis is performed on a bare sphere benchmark consisting of a homogeneous mixture UF_4 and polyethylene [7]. And the results computed by the RMC integrated built-in stochastic sampling module (RMC-SS) are compared by TSUNAMI-3D in the SCALE 6.1 code package and RMC previous sensitivity module which is based on iterated fission probability (IFP) method. Both TSUNAMI-3D and RMC-IFP are based on the sensitivity/uncertainty method. TSUNAMI-3D is based on a 3D multi-group Monte Carlo code KENO while RMC is continuous-energy Monte Carlo code.

RMC uses the ENDF/B-VII.0 continuous-energy cross section library as the nominal data library while the 44-group covariance data library of SCALE6.1 as the perturbed library.

Fig. 4 shows the probability density function of k_{eff} where the ^{238}U capture cross section (MT=102) are perturbed. As shown, the probability density function of k_{eff} fits well with Gaussian distribution (normal distribution).

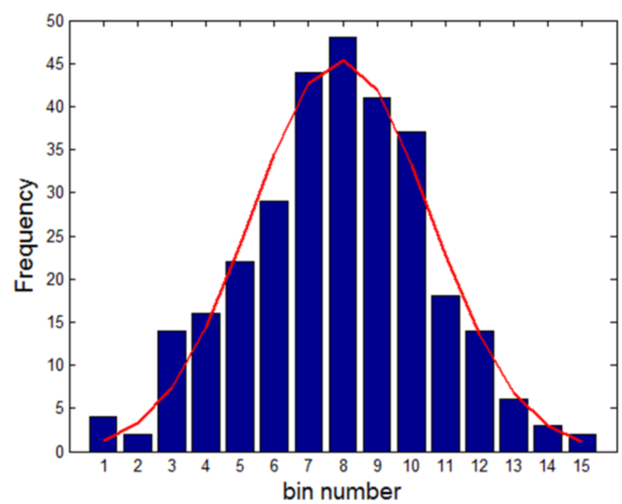

Fig. 4. Probability density function of k_{eff} calculated by RMC

Table 1 presents the uncertainties calculated by RMC-SS, RMC-IFP and TSUNAMI-3D. The difference in Table 1 is defined as the RMC-SS uncertainty from nuclear data divided by the corresponding RMC-IFP result.

RMC-IFP uses 500,000 particles × 20,000 active cycles plus 250 inactive cycles while RMC-SS uses 10,000 particles × 10,000 active cycles plus 250 inactive cycles for each run. And 300 repeated runs are required to obtain one uncertainty data for the RMC-SS method. According to Table 1, 16 different uncertainty data are obtained.

Therefore, the total number of particles in the active cycles is 480,000,000,000 for the RMC-SS method and 10,000,000,000 for the RMC-IFP method, which means the RMC-SS method requires 47 times of computational efforts more than the RMC-IFP method.

However, it should be noted some of differences between the RMC-SS method and the RMC-IFP method are larger than 20%. The main reason is probably due to the difference between the sensitivity/uncertainty method and the stochastic sampling method. The sensitivity/uncertainty method is based on the assumption that the relationship between the output and the input is linear. In the stochastic sampling method, in order to decompose the relative covariance data library V in the form of Eq. 1, V has to be modified to be a symmetric positive define matrix or a symmetric positive semi-define matrix since the original V is not.

Another reason is the statistical uncertainty is still large, which is around $50\% \times \sigma_{observed}$, such as the ^{235}U inelastic cross section (MT=4).

2. Burnup Calculation

Uncertainty analysis is performed on the OECD LWR UAM Exercise I (I -1) -I-1b (Cell Burn-up Physics) which is address the uncertainties in the depletion calculation due to the basic nuclear data as well as the impact of processing of nuclear and covariance data [1]. The configuration of this pin-cell is presented in Fig. 5, which is plotted by RMC.

The benchmark is used to evaluate uncertainties of k_{eff}, reactions and collapsed cross-sections, and nuclide concentrations in the depletion. The specific power is 25 kW/kgU and the final burn-up is 61.28 GWd/MTU.

RMC uses the ENDF/B-VII.0 continuous-energy cross section library as the nominal data library while the 44-group covariance data library of SCALE6.1 as the perturbed library.

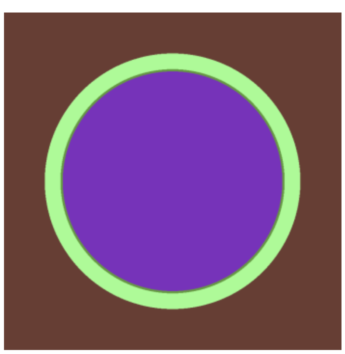

Fig. 5. Configuration of PWR burnup pin-cell benchmark

The stochastic sampling method is used to obtain most of the uncertainties, except the uncertainty breakdown which is calculated by the sensitivity/uncertainty method.

RMC-IFP uses 200,000 particles × 10,000 active cycles plus 100 inactive cycles while RMC-SS uses 10,000 particles × 250 active cycles plus 50 inactive cycles for each run. And 300 repeated runs are performed for the RMC-SS method.

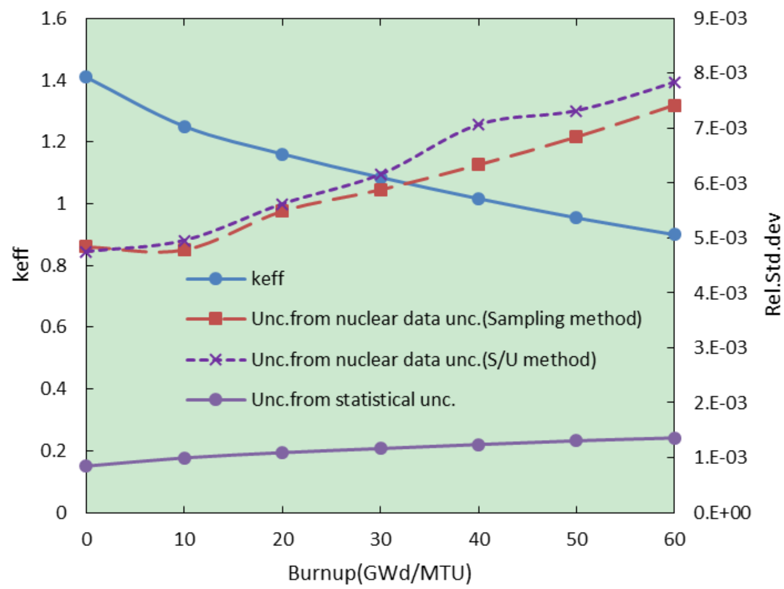

Fig. 6. k_{eff} uncertainty versus burnup.

Fig. 6 shows k_{eff} and its uncertainties (in forms of relative standard deviations, σ_k / k) due to nuclear data uncertainties as well as Monte Carlo statistical uncertainties. As shown in Fig. 6, the uncertainties in k_{eff} from statistical uncertainties are much smaller than the uncertainties in k_{eff} from nuclear data uncertainties. And the relative standard deviation of k_{eff}, increases with burnup since the k_{eff} decreases and the number of isotopes increases. It should be noted that the uncertainty calculated by the sensitivity/uncertainty method (RMC-IFP) is larger than the corresponding uncertainty calculated by the stochastic sampling method (RMC-SS). Since the sensitivity/uncertainty method does not consider the propagation of the uncertainty of isotopic density, it can be asserted that the nuclear data and the isotopic density may have a negative correlation and the uncertainties calculated by the sensitivity/uncertainty method is conservative.

Table 2 lists top five nuclear data in terms of contribution to uncertainties in k_{eff} before shutdown while Table 3 lists top five nuclear data in terms of contribution to uncertainties in k_{eff} after shutdown. As shown in Table 2, at the initial burnup step, ^{235}U average fission neutron number (nubar, MT=452) contributes the most of the uncertainties in k_{eff} while ^{238}U capture cross section (MT=102) contributes the most of the uncertainties in k_{eff} at

10 GWd/MTU. As burnup increases, ^{239}Pu average fission neutron number (nubar, MT=452) becomes the first contributor of uncertainties in k_{eff}. As shown in Table 3, the ranking remains almost the same from the shutdown till 100 years.

As can be seen, at the initial burnup step, ^{235}U average fission neutron number (nubar, MT=452) contributes the most of the uncertainties in k_{eff} while ^{238}U capture cross section (MT=102) contributes the most of the uncertainties in k_{eff} at 10 GWd/MTU. As burnup increases, ^{239}Pu average fission neutron number (nubar, MT=452) becomes the first contributor of uncertainties in k_{eff}.

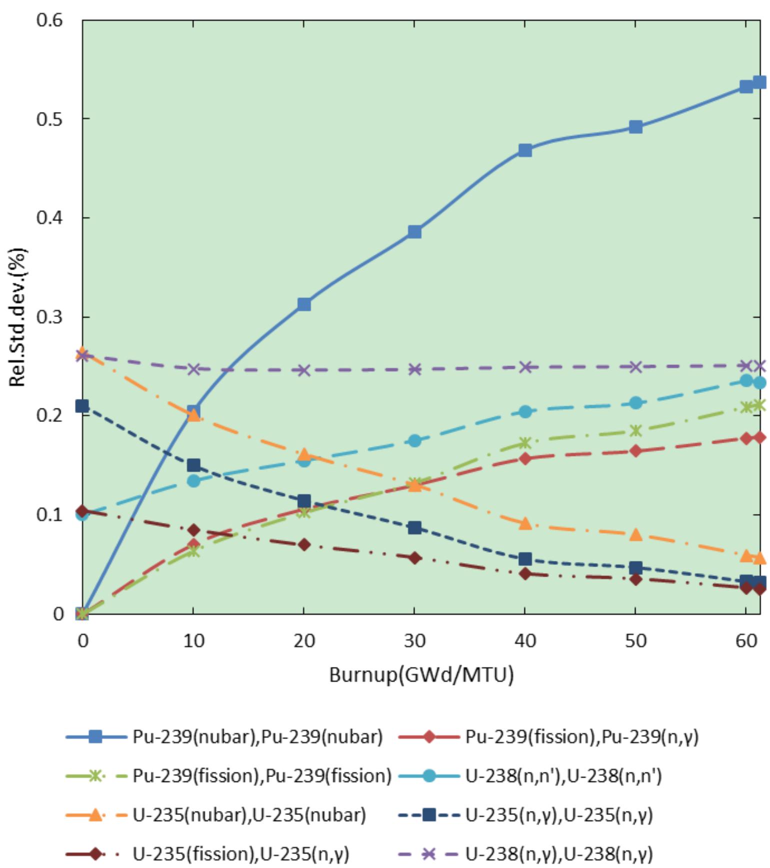

Fig. 7. Relative standard deviations of k_{eff} due to uncertainties of some important reaction pairs.

Fig. 7 presents the relative standard deviations of k_{eff} due to those reaction pairs lists in Table 2. In the initial burnup step, U-235 (nubar) to U-235 (nubar) and U-238 (n, γ) to U-238 (n, γ) are the two biggest uncertainty sources. The uncertainty from reaction pair U-235 (nubar) to U-235 (nubar) decreases with burnup since the U-235 number density decreases while the uncertainty from reaction pair U-238 (n, γ) to U-238 (n, γ) almost remains unchanged since the U-238 number density changes slowly. And the reaction pair, Pu-239 (nubar) to Pu-239 (nubar), increases its contribution to uncertainties in k_{eff} with burnup and becomes the biggest uncertainty source at high burup.

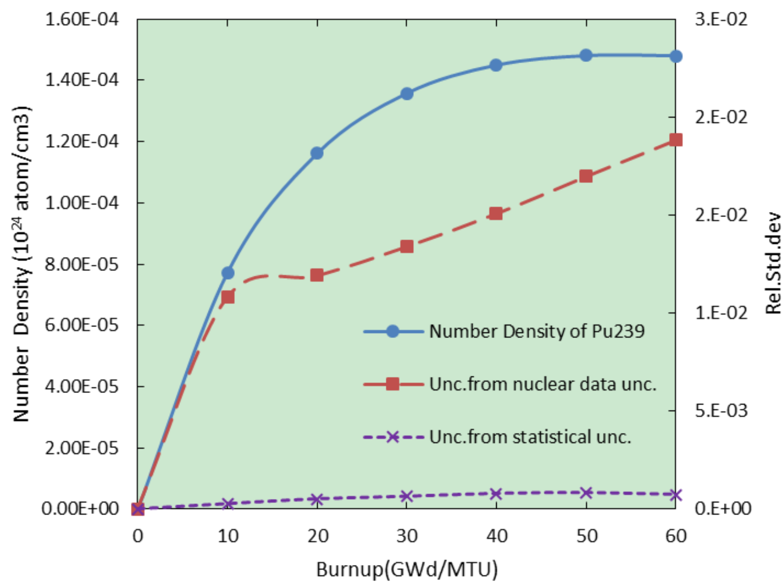

Fig. 8. Relative standard deviations of ^{239}Pu number density versus burnup.

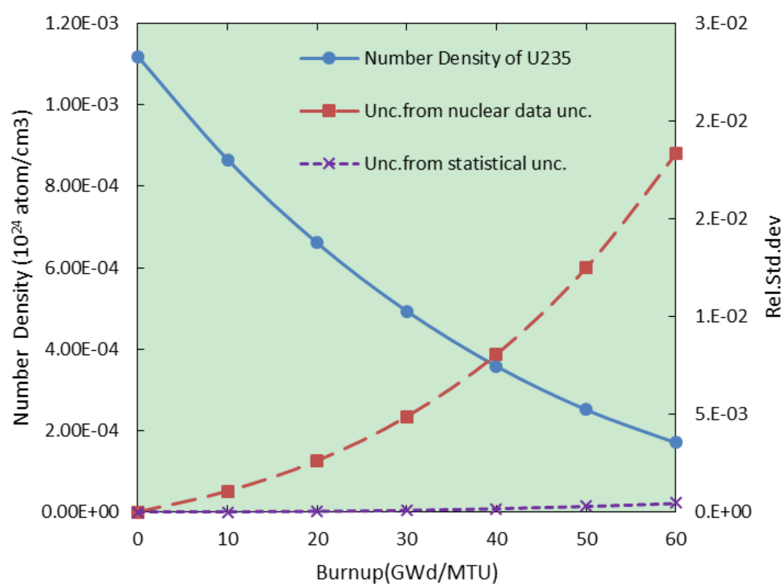

Fig. 9. Relative standard deviations of ^{235}U number density versus burnup.

Fig. 8 shows the uncertainty in ^{239}Pu number density versus burnup. As can been seen, the uncertainties in ^{239}Pu number density from statistical uncertainties are much smaller than the uncertainties from nuclear data uncertainties. And both the relative standard deviation of ^{239}Pu number density due to statistical uncertainties and that due to nuclear data, increase with burnup.

Fig. 9 shows the uncertainty in ^{235}U number density versus burnup. As can been seen, the uncertainties in ^{235}U number density from statistical uncertainties are much smaller than the uncertainties from nuclear data uncertainties. And the relative standard deviation of ^{235}U number density due to statistical uncertainties and that due to nuclear data, increase with burnup.

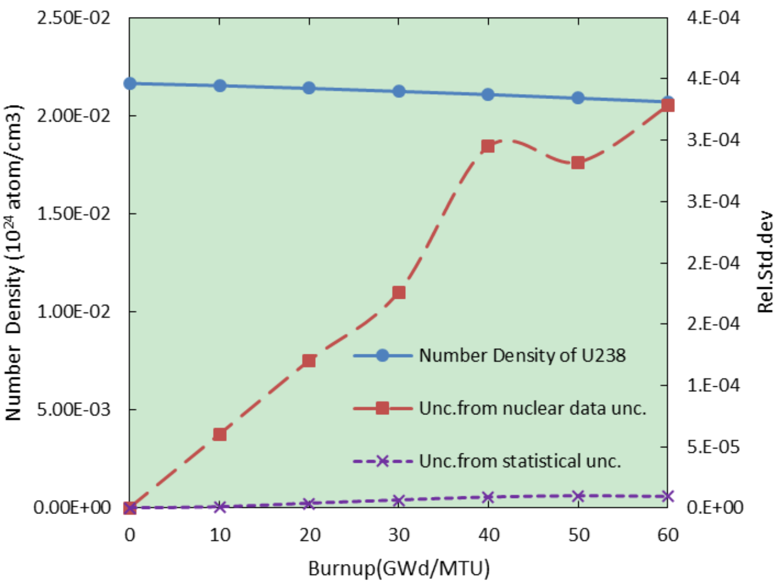

Fig. 10. Relative standard deviations of ^{238}U number density versus burnup.

Fig. 10 shows the uncertainty in ^{238}U number density versus burnup. As can been seen, the uncertainties in ^{238}U number density from statistical uncertainties are much smaller than the uncertainties from nuclear data uncertainties. And the relative standard deviation of ^{238}U number density due to statistical uncertainties and that due to nuclear data, increase with burnup. It is also noted that the uncertainties increase before 40 Gwd/MTU and deceases after 40 Gwd/MTU. More burnup steps should be inserted between 30 Gwd/MTU and 50 Gwd/MTU to find out the reason.

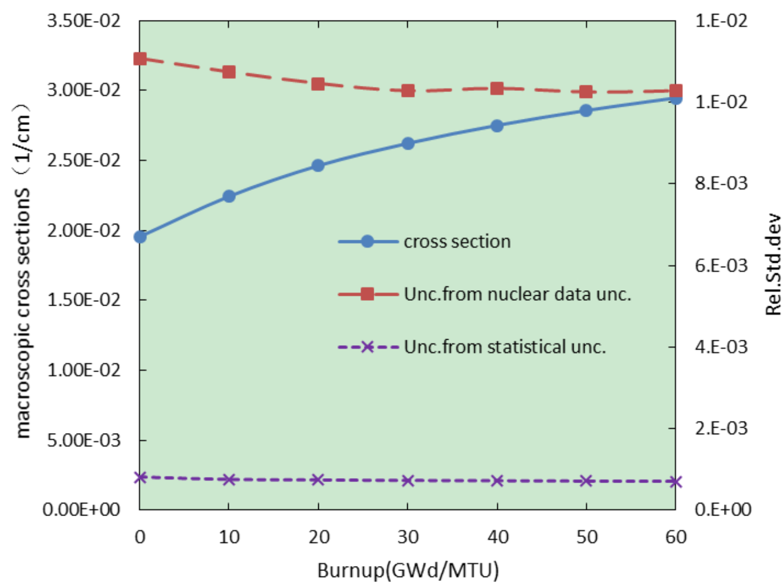

Fig. 11. Relative standard deviations of fuel-only, macroscopic absorption cross section for fast group versus burnup.

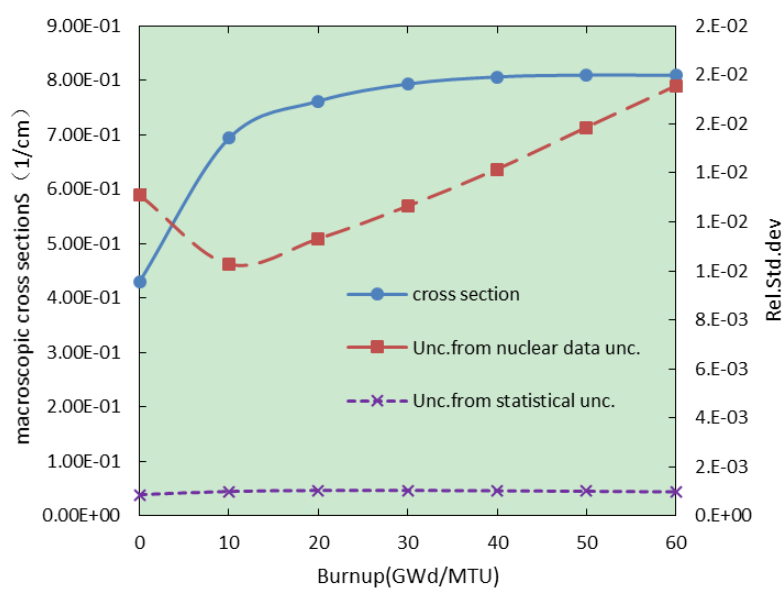

Fig. 12. Relative standard deviations of fuel-only, macroscopic absorption cross section for thermal group versus burnup.

Figs. 11 and 12 show uncertainty of fuel-only, macroscopic absorption cross section for fast group and thermal group respectively. As shown in Figs. 11 and 12, the uncertainties from statistical uncertainties are much smaller than the uncertainties from nuclear data uncertainties. Both the macroscopic absorption cross section for fast group and that for thermal group increase with burnup. The uncertainty in the macroscopic absorption cross section for fast group due to nuclear data decreases while that for thermal group due to nuclear data drops at the low burnup steps and raises at the high burnup steps.

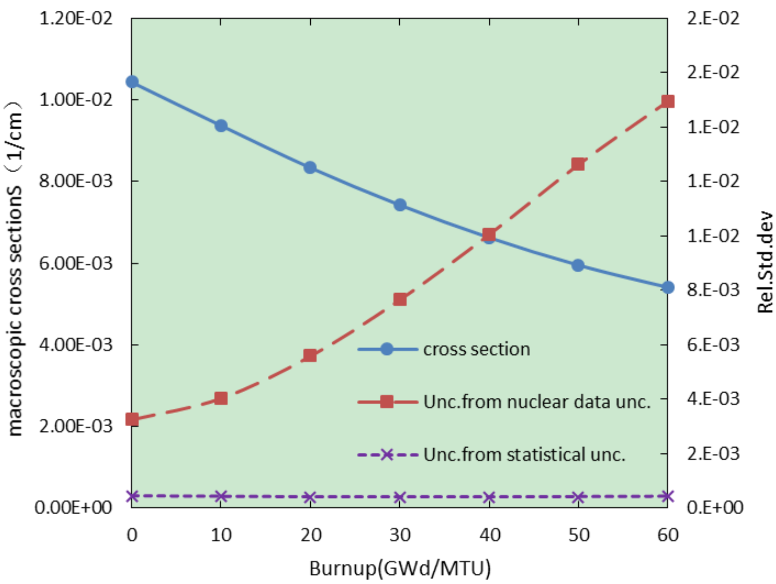

Fig. 13. Relative standard deviations of fuel-only, macroscopic fission cross section for fast group versus burnup.

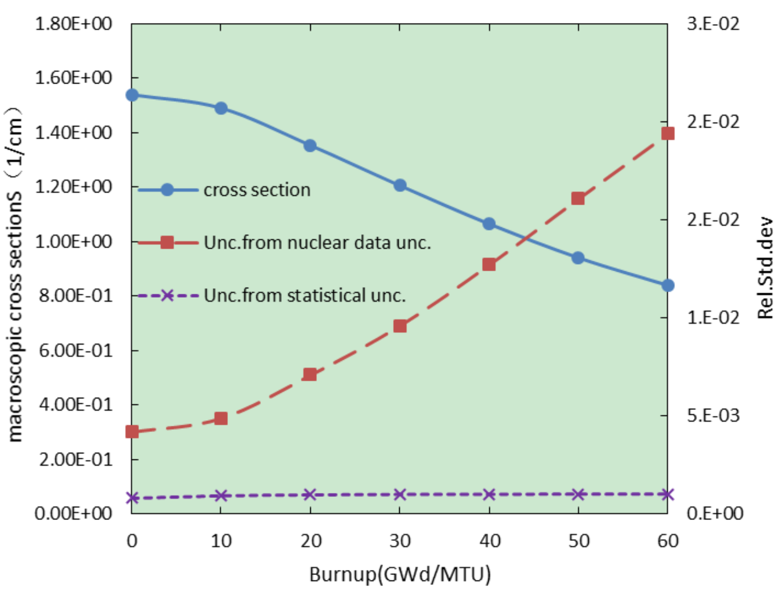

Fig. 14. Relative standard deviations of fuel-only, macroscopic fission cross section for thermal group versus burnup.

Figs. 13 and 14 show uncertainty of fuel-only, macroscopic fission cross section for fast group and thermal group respectively. As shown in Figs. 13 and 14, the uncertainties from statistical uncertainties are much smaller than the uncertainties from nuclear data uncertainties. Both the macroscopic fission cross section for fast group and that for thermal group decrease with burnup. Both the uncertainty in the macroscopic absorption cross section for fast group and the thermal group due to nuclear data increase with burnup.

IV. CONCLUSIONS

Provide the conclusions of the work. In this paper, an integrated, built-in stochastic sampling module, RMC-SS, was developed based on the Reactor Monte Carlo code RMC. Comparing to the traditional stochastic sampling tool which takes the transport code as a black box, RMC-SS is much more user-friendly. Instead of perturbed nuclear data library, perturbation factors are prepared and stored, which can reduce memory consumption of storing library. After reading nominal library and perturbation factors, RMC automatically repeats transport or burnup calculations. Finally, uncertainties of results are calculated by RMC. No post processing is required. The RMC-SS tool has been applied in two problems, a bare sphere benchmark and a PWR pin cell burnup benchmark, to perform uncertainty analysis in Monte Carlo transport calculation and burnup calculation.

ACKNOWLEDGMENTS

The authors wish to thank Dr. Manuele Aufiero from University of California, Berkeley and Dr. Ting Zhu from Paul Scherrer Institute provide fruitful discussion about the PSI sampling process.

REFERENCES

1. K. Ivanova, M. Avramova, S. Kamerow, et al.,, “Benchmark For Uncertainty Analysis in Modeling (UAM) For Design, Operation and Safety Analysis of LWRs,” NEA/NSC/DOC (2013).
2. Y. Qiu, M. Aufiero, K. Wang, M. Fratoni, “Development of Sensitivity Analysis Capabilities of Generalized Responses to Nuclear Data in Monte Carlo Code RMC,” *Annals of Nuclear Energy*, 97, 142–152 (2016).
3. D. Rochman, W. Zwermann, S.C. van der Marck, et al., “Efficient use of Monte Carlo: uncertainty propagation,” *Nuclear Science and Engineering*, 177(3), 337-349 (2016).
4. T. Zhu, et al., “NUSS: A tool for propagating multigroup nuclear data covariances in pointwise ACE-formatted nuclear data using stochastic sampling method,” *Annals of Nuclear Energy*, 75, 713–722 (2015).
5. W. Wieselquist, A. Vasiliev, and H. Ferroukhi, “Nuclear data uncertainty propagation in a lattice physics code using

stochastic sampling," *Proc. PHYSOR 2012*, Knoxville, Tenn, USA, April 15–20, 2012, American Nuclear Society (2012).
6. W. ZWERMANN et al., "Aleatoric and Epistemic Uncertainties in Sampling Based Nuclear Data Uncertainty and Sensitivity Analyses,'' *Proc. PHYSOR 2012*, Knoxville, Tenn, USA, April 15–20, 2012, American Nuclear Society (2012).
7. B.T. Rearden, "Perturbation Theory Eigenvalue Sensitivity Analysis with Monte Carlo Techniques," *Nucl. Sci. Eng.*, 146, 367 (2004).

Table 1. Comparison of the relative standard deviation of keff ($\%\Delta k / k$) due to cross-section covariance data for polyethylene sphere

Nuclide	MT	Nuclide	MT	S/U method（%）		RMC-SS（%）			RMC-SS/ RMC-IFP
				TSUNAMI-3D	RMC-IFP	ND	MC	Total	
1001	2	1001	2	1.170E-01	1.169E-01	1.096E-01	6.900E-03	1.098E-01	0.94
1001	102	1001	102	5.065E-02	4.979E-02	4.560E-02	6.900E-03	4.610E-02	0.92
6000	2	6000	2	1.543E-02	1.568E-02	1.660E-02	6.900E-03	1.800E-02	1.06
9019	2	9019	2	1.353E-01	1.331E-01	1.295E-01	6.900E-03	1.297E-01	0.97
9019	4	9019	4	1.111E-01	1.124E-01	1.101E-01	6.900E-03	1.103E-01	0.98
9019	107	9019	107	1.949E-02	1.961E-02	1.950E-02	6.900E-03	2.070E-02	0.99
92235	452	92235	452	2.851E-01	2.847E-01	2.593E-01	6.900E-03	2.594E-01	0.91
92235	102	92235	102	1.595E-01	1.573E-01	1.536E-01	6.900E-03	1.538E-01	0.98
92235	18	92235	18	1.220E-01	1.231E-01	1.100E-01	6.900E-03	1.102E-01	0.90
92235	4	92235	4	1.352E-03	1.407E-03	5.000E-03	6.900E-03	8.600E-03	3.55
92238	102	92238	102	3.859E-01	3.777E-01	3.311E-01	6.900E-03	3.311E-01	0.88
92238	4	92238	4	2.156E-01	2.274E-01	9.620E-02	6.900E-03	9.640E-02	0.42
92238	452	92238	452	5.851E-02	5.945E-02	6.270E-02	6.900E-03	6.310E-02	1.05
92238	2	92238	2	6.894E-02	4.840E-02	4.810E-02	6.900E-03	4.860E-02	0.99
92238	18	92238	18	1.735E-02	1.770E-02	4.830E-02	6.900E-03	4.880E-02	2.78
92238	16	92238	16	1.353E-02	1.316E-02	4.000E-03	6.900E-03	8.000E-03	0.30

Table 2. Top five nuclear data in terms of contribution to uncertainties in k_{eff} before shutdown

ranking	0 GWd/MTU	10 GWd/MTU	20 GWd/MTU	30 GWd/MTU	40 GWd/MTU	50 GWd/MTU	60 GWd/MTU	61.28 GWd/MTU
1	mt452_92235	mt102_92238	mt452_94239	mt452_94239	mt452_94239	mt452_94239	mt452_94239	mt452_94239
2	mt102_92238	mt452_94239	mt102_92238	mt102_92238	mt102_92238	mt102_92238	mt102_92238	mt102_92238
3	mt102_92235	mt452_92235	mt452_92235	mt4_92238	mt4_92238	mt4_92238	mt4_92238	mt4_92238
4	(mt18_92235, mt102_92235)	mt102_92235	mt4_92238	mt18_94239	mt18_94239	mt18_94239	mt18_94239	mt18_94239
5	mt4_92238	mt4_92238	mt102_92235	mt452_92235	(mt102_94239, mt18_94239)	(mt102_94239, mt18_94239)	(mt102_94239, mt18_94239)	(mt102_94239, mt18_94239)

Table 3. Top five nuclear data in terms of contribution to uncertainties in k_{eff} after shutdown

ranking	1 year	3 years	5 years	10 years	50 years	100 years
1	mt452_94239	mt452_94239	mt452_94239	mt452_94239	mt452_94239	mt452_94239
2	mt102_92238	mt102_92238	mt102_92238	mt102_92238	mt102_92238	mt102_92238
3	mt4_92238	mt4_92238	mt4_92238	mt4_92238	mt4_92238	mt4_92238
4	mt18_94239	mt18_94239	mt18_94239	mt18_94239	mt18_94239	mt18_94239
5	(mt102_94239, mt18_94239)	(mt102_94239, mt18_94239)	(mt102_94239, mt18_94239)	(mt102_94239, mt18_94239)	(mt102_94239, mt18_94239)	mt-1018_94239